

Ensemble Neural Networks for Remaining Useful Life (RUL) Prediction

Abhishek Srinivasan

Connected Systems, Scania CV AB, Södertälje, Sweden
KTH Royal Institute of Technology, Stockholm, Sweden
RISE Research Institutes of Sweden, Stockholm, Sweden
abhishek.srinivasan@scania.com

Juan Carlos Andresen

Connected Systems, Scania CV AB, Södertälje, Sweden
juan-carlos.andresen@scania.com

Anders Host

RISE Research Institutes of Sweden, Stockholm, Sweden
KTH Royal Institute of Technology, Stockholm, Sweden
anders.holst@ri.se

Abstract—A core part of maintenance planning is a monitoring system that provides a good prognosis on health and degradation, often expressed as remaining useful life (RUL). Most of the current data-driven approaches for RUL prediction focus on single-point prediction. These point prediction approaches do not include the probabilistic nature of the failure. The few probabilistic approaches to date either include the aleatoric uncertainty (which originates from the system), or the epistemic uncertainty (which originates from the model parameters), or both simultaneously as a total uncertainty. Here, we propose ensemble neural networks for probabilistic RUL predictions which considers both uncertainties and decouples these two uncertainties. These decoupled uncertainties are vital in knowing and interpreting the confidence of the predictions. This method is tested on NASA’s turbofan jet engine CMAPSS data-set. Our results show how these uncertainties can be modeled and how to disentangle the contribution of aleatoric and epistemic uncertainty. Additionally, our approach is evaluated on different metrics and compared against the current state-of-the-art methods.

I. INTRODUCTION

The cost of downtime due to failure and its corresponding unplanned maintenance is high. A well-planned maintenance strategy can better minimize these failure occurrences. Predictive maintenance (an advanced maintenance planning strategy) uses models to monitor the health index of a system to schedule a maintenance. A popular health index is the Remaining Useful Life (RUL), which is the effective life left of a component measured in number of operational time, such as number of cycles, number of hours, or amount of air pumped. The two main streams of RUL modeling approaches are physics based and data-driven based. **Physics based** models are mathematical representations of a system degradation to predict RUL. For complex systems, one common method for RUL modeling is to divide the system into subsystems and recurrently modeling its sub-components individually [1]. This process of decomposing the system into smaller sub-systems and modeling them can be repeated until the desired level of

granularity is reached. This granularity selection also affects the accuracy of the model (in general, the deeper the level of granularity, the more accurate the model is). This modeling approach can be time-consuming and deep domain knowledge about the system and sub-systems is needed. **Data-driven** models are modeled using data obtained from the system. With the developments in machine learning (ML) the process of data-driven modeling has become more accurate than ever [2]. Motivated by the success of deep learning (DL) in computer vision and text processing [2], [3] DL has become mainstream among many researchers within PHM. Currently, state-of-the-art models take two different directions for RUL modeling for complex systems; on one hand the inputs are directly mapped onto the RUL [4], [5] and on the other hand, when a health index is possible to be defined or measured, the modeling is done in a two step procedure *i*) inputs are mapped onto the health index, *ii*) the health index is mapped onto the RUL [6]. Despite the good accuracy of the current approaches using DL [4]–[6], most of them model point estimates of the RUL without considering the probabilistic nature of the system and uncertainties in the modeling [5].

In general, there are two main sources of uncertainties in the modeling process; *aleatoric uncertainty* which is originated from the system failing at different operational times, and *epistemic uncertainty* which comes from uncertainties of the model parameters, e.g. these model parameters might change with the quantity of available data. Knowing the source of the uncertainties gives the possibility of taking better decisions based on the model predictions [7]. For instance, when the epistemic uncertainties are large the model predictions should not be trusted. This high epistemic uncertainty strongly indicates that the provided input is different than the trained data distribution. If the aleatoric uncertainties dominate, then the uncertainties are inherent to the underlying system (or quality of data) and cannot be reduced by adding any other source of information. For industrial applications, being able

to distinguish between these uncertainties can be of much help, i.e., *i*) the aleatoric uncertainty provides information about the variance in the failure process. This information can be used to know the amount of risk taken when planning the maintenance. *ii*) the high epistemic uncertainty indicates regions where more data collection is needed to enrich model’s knowledge. This distinction gives crucial information to interpret the model output more accurate in relation to the uncertainties, thus improving the trustworthiness.

In this work, we predict the probabilistic estimates; incorporating the aleatoric and the epistemic uncertainties by utilizing an ensemble neural network. This ensemble based approach is simple, easily parallelizable, and well calibrated to reflect real underlying behavior. Our methods are tested on NASA’s turbofan jet engine CMAPSS data-set benchmark [8]. The results show the capability of our model approach to provide probabilistic estimates and can measure the isolated effect of the aleatoric and epistemic uncertainties.

The paper begins with related work followed by ensemble neural networks for probabilistic modeling, then we describe the experiments and results. Finally, we show some advantages of this method and conclude this work.

II. RELATED WORK

A number of different authors use neural networks to predict the RUL of a system. The most common neural network architectures for this application are Convolution Neural Networks (CNN) and Long Short-term Memory (LSTM). [4] use an LSTM network combined with fully connected layers that take in normalized data and predict RUL. [5] use CNN with attention mechanism to the predict the RUL along with some interpretability methods. The aforementioned approaches model for point prediction, our work aims to model probabilistic predictions incorporating uncertainties.

Some work that considers probabilistic prediction are [6]; [9]; [10]; [11]. The work of [6] uses three-step model for probabilistic RUL prediction. The first step is to predict the probability distribution health index. In the second step, the predicted distribution of the health index is mapped onto the RUL estimated distribution. The third step is a correction carried out using LSTMs, this step acts as a re-calibrator for the prediction. Although the uncertainty estimation on the NN is similar to our work, one crucial difference between this work and Nemani’s work is that our method is a single-stage prediction where inputs are mapped directly onto the RUL. This is important in complex systems such as CMAPSS where defining a health index that is interpretable and observable is difficult or even impossible.

[11] use Monte Carlo dropout approach for probabilistic predictions and it requires high computation and modeling time compared to our approach [12]. [10] use an approach of modeling which only takes into account uncertainties from the system and does not model the uncertainties of model parameters. Another approach by [9] where they measure the uncertainties from the model (epistemic) and don’t consider the uncertainties from the system (aleatoric).

Most of the existing work focuses on modeling point prediction for the RUL and only a few focus on probabilistic methods. To our knowledge the existing probabilistic methods either estimate the aleatoric, or the epistemic uncertainties, or both simultaneously without separating the source of uncertainties. Our approach models a probabilistic approach that distinguishes the source of uncertainties.

III. METHODS

A. Ensemble Neural Networks for Prediction

[12] proposed a novel approach to model both aleatoric and epistemic uncertainties using deep ensembles probabilistic networks. Individuals of an ensemble are made of probabilistic neural networks (PNN). This PNN is a probabilistic model which captures aleatoric uncertainties from a given data. PNNs work like a neural network with the difference that they predict the parameters θ of the assumed distribution $\Pi(\theta)$. Additionally, epistemic uncertainties are captured by the ensembles, by the fact that individuals in the ensemble converges to different optimums while capturing the distribution of the model parameters. During the training process, the optimizer aims to find parameters for the PNN to maximize the selected scoring rule.

The *Scoring rule* is a function that measures the quality of the predicted distribution p_θ . The higher the value is, the better the quality of prediction is. This scoring rule helps to check if the model is calibrated *i.e.*, the predicted distribution p_θ reflects the real distribution q , where θ is the parameter of the assumed distribution. A well-defined scoring rule should satisfy the following conditions: *i*) $S(p_\theta, Y|x) < S(q, Y|x)$ and *ii*) $S(p_\theta, Y|x) = S(q, Y|x)$ if and only if $p_\theta(Y|x) = q(Y|x)$. Negative log likelihood (NLL) and Brier score are some examples of scoring rules that satisfy the above properties.

B. Proposed Model Structure

The proposed model uses a Gaussian distribution $\mathcal{N}(\mu, \sigma)$ as the assumed distribution $\Pi(\theta)$, where μ is the mean and σ is the standard deviation. In other words, the distribution of the RUL estimates is assumed to be Normal distributed. The model architecture consists of K stacks of LSTM layers followed by L fully connected layers which output two parameter estimates $\hat{\mu}$ and $\hat{\sigma}$. This network is trained using the NLL of the Gaussian distribution, and the training data is used as observations on the predicted distribution. The NLL of the i^{th} sample is given by Eq. (1). Our modeling approach predicts the RUL at every time step of the provided window.

$$-\log \mathcal{P}_{\mu, \sigma}(y_i | \mathbf{x}_i) = \frac{\log \sigma^2(\mathbf{x}_i)}{2} + \frac{(y_i - \mu(\mathbf{x}_i))^2}{2\sigma^2(\mathbf{x}_i)} + \text{const.} \quad (1)$$

The prediction from M individuals of ensembles is put together by finding the mean distribution $\mathcal{N}(\hat{\mu}_*, \hat{\sigma}_*)$

$$\hat{\mu}_* = \frac{1}{M} \sum_{i=1}^M \hat{\mu}_i, \quad (2)$$

$$\hat{\sigma}_*^2 = \frac{1}{M} \sum_{i=1}^M (\hat{\sigma}_i^2 + \hat{\mu}_i^2) - \hat{\mu}_*^2. \quad (3)$$

C. Uncertainty Measures

As mentioned before the total uncertainty can be split into aleatoric and epistemic, which can be expressed as $U_{tot} = U_{al} + U_{ep}$. Aleatoric uncertainty can be measured by the average entropy H of each prediction, this is $U_{al} = \frac{1}{M} \sum_{i=1}^M H(\mathbf{p}^{(i)})$, where M is the total number of models in the ensemble, i is an individual in the ensemble and $\mathbf{p}^{(1)}, \dots, \mathbf{p}^{(M)}$ are the M predictive distributions of the ensemble. The total uncertainty U_{tot} can be calculated as the entropy of the mean prediction, i.e., $U_{tot} = H(\frac{1}{M} \sum_{i=1}^M \mathbf{p}^{(i)})$. Therefore, $U_{ep} = H(\frac{1}{M} \sum_{i=1}^M \mathbf{p}^{(i)}) - \frac{1}{M} \sum_{i=1}^M H(\mathbf{p}^{(i)})$ [13]. By assuming a Normal distributed variable, i.e., $x \sim \mathcal{N}(\mu, \sigma)$, the entropy can be expressed as $H = \frac{1}{2} \log(2\pi\sigma^2) + \frac{1}{2}$. Therefore, $U_{tot} = \frac{1}{2} \log(2\pi\hat{\sigma}_*^2) + \frac{1}{2}$ and we can write the *aleatoric* and *epistemic* uncertainties as

$$U_{al} \sim \frac{1}{M} \sum_{i=1}^M \log(\hat{\sigma}_i^2), \quad (4)$$

$$U_{ep} \sim \log(\hat{\sigma}_*^2) - \frac{1}{M} \sum_{i=1}^M \log(\hat{\sigma}_i^2). \quad (5)$$

IV. EXPERIMENTAL SETTING

A. Data

Our proposed method was tested on NASA's turbofan jet engine CMAPSS data-set [8], specifically using FD001 for training and test sets form FD001, FD002 and FD003 data-sets. These data-sets were curated for RUL prediction tasks, containing 21 selected signals collected during different operational cycles until failure. we omitted sensor signals 1, 5, 10, 16, 18, and 19 as their values are constant in data-set FD001. We utilize piecewise linear RUL targets; in the initial stages we assume the RUL to be a constant of value 128 and linearly decreasing in the last 128 cycles, similar to previous approaches [10], [14].

TABLE I: Table summarizing the NASA turbofan jet engine data-set. This consists of four data-set with different number of units, operating conditions, and fault modes.

	FD001	FD002	FD003	FD004
Train Units	100	260	100	249
Test Units	100	259	100	249
Operating Condition	1	6	1	6
Fault Modes	1	1	2	2

The data is pre-processed, where the signals are normalized using the Z -norm $x_i^{norm} = (x_i - \mu_x)/\sigma_x$. The normalizing

parameters of the train data are utilized for normalizing the test. Additionally, the sliding window method is used to generate samples that are used as inputs to the neural networks. This is typically done by using a window of length l and this window is moved along time on stride s . For this work, the stride s was set to 1 and the window length l was set to 100.

B. Model

For reproducibility purposes, the experiments utilized a fixed random seed 237. Our model uses 2 layers of LSTM layers each with 32 and 16 neurons, respectively. LSTM layers are followed by 1 dense layer. Our ensemble consists of 15 models. Train and test split is according to the original data-set. Our models utilize a batch-size of 32 and an Adam optimizer with a learning rate of $\lambda = 0.001$, parameters $\beta_1 = 0.9$, and $\beta_2 = 0.999$. An early stopping mechanism monitors loss from epoch 35 and waits for 3 epochs to cut off the training when loss continues to increase or at 100 epochs.

C. Evaluation Metric

In order to compare against the point prediction methods, we evaluate our method against the same metrics that are used in point prediction methods. For this purpose, the mean measure is calculated. Commonly used metric for point predictions are Root Mean Square Error (RMSE) shown in Eq. (6), where N is the number of samples in the data-set and \hat{y} is the model prediction. The Score function is shown in Eq. (7) where a_1 is set to 10 and a_2 to 13 as in [8].

$$RMSE = \sqrt{\frac{1}{N} \sum_{i=1}^N (\hat{y}_i - y_i)^2} \quad (6)$$

$$s = \begin{cases} \sum_{i=1}^N e^{-\left(\frac{\hat{y}_i - y_i}{a_1}\right)} - 1 & \text{for } (\hat{y}_i - y_i) < 0 \\ \sum_{i=1}^N e^{\left(\frac{\hat{y}_i - y_i}{a_2}\right)} - 1 & \text{for } (\hat{y}_i - y_i) \geq 0 \end{cases} \quad (7)$$

For evaluating the probabilistic predictions, we use the prediction interval coverage percentage (PICP) and normalized mean prediction interval width (NMPIW). PICP measures the percent of the prediction which falls within the bounds given the confidence interval. NMPIW measures the average width of the bounds, i.e., upper and lower-bound in a possible range of values. Formulae for PICP and NMPIW are provided in Eq. (8) and Eq. (9), respectively,

$$PICP = \frac{1}{N} \sum_{i=1}^N \begin{cases} 1 & \text{if } y_i \in [U_\alpha(\hat{\mathbf{p}}_i), L_\alpha(\hat{\mathbf{p}}_i)] \\ 0 & \text{if } y_i \notin [U_\alpha(\hat{\mathbf{p}}_i), L_\alpha(\hat{\mathbf{p}}_i)] \end{cases}, \quad (8)$$

$$NMPIW = \frac{1}{N(\max\{y\} - \min\{y\})} \sum_{i=1}^N (U_\alpha(\hat{\mathbf{p}}_i) - L_\alpha(\hat{\mathbf{p}}_i)), \quad (9)$$

where $\hat{\mathbf{p}}_i$ is the estimated distribution by the i^{th} individual in the ensemble. The upper bound $U_\alpha(\mathbf{p})$ and lower bound $L_\alpha(\mathbf{p})$ are calculated based on the confidence interval α of the distribution \mathbf{p} . We use a 95% confidence interval for our calculations.

V. RESULTS AND DISCUSSION

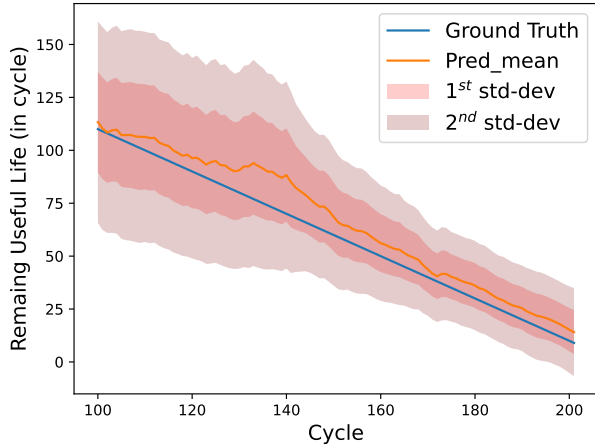


Fig. 1: Prediction of unit 34 from the test set in FD001 using model trained on train set form FD001. Here the predictions are for the last 102 window steps.

In our modeling process, we train by using a window of 100 time steps and predict all 100 time steps. Usually, RUL models are evaluated by the prediction done at the last available time step, therefore we utilize only the last time step to compare with existing models. Prediction for one test unit can be seen in the Fig. 1, the mean prediction follows the ground truth and variance decreases later in the operational life of this random unit.

We train the ensemble model on the folder FD001 and calculated the aleatoric and epistemic uncertainty for all the samples in test-sets from folders FD001, FD002, and FD003. The kernel density estimate of the aleatoric and epistemic uncertainties are plotted in Fig. 2 (a) and Fig. 2 (b), respectively. From Fig. 2 (b), it is clear that the epistemic uncertainties for the samples from FD002 are high compared to the samples in FD001. This high uncertainty indicates that the model has not been trained on the data distribution of FD002 and should not be trusted (*i.e.*, re-training needed for this data-set). In the case of FD003 the ensemble model has an epistemic uncertainty that is closer to the FD001, indicating that the prediction can be trusted but are not as good as for FD001 and data-distribution is closer to FD001. To further analyze the epistemic uncertainty and how this reflects on the difference in data distribution of the different data-sets (*i.e.*, FD001, FD002 and FD003), we plot in Fig. 2 (c) the T-distributed stochastic neighbor embedding (TSNE), a dimensionality reduction technique on the data-space of FD001, FD002 and FD003. This visualization shows the data embedding of the different data-sets, one can see that the FD001 are subsets of FD002, and that FD003 is majorly a sub-set of FD001 with minor exceptions that can be seen on the left boundaries. Fig. 2 (c) confirms our interpretation of the epistemic uncertainty in data-set FD002 and FD003.

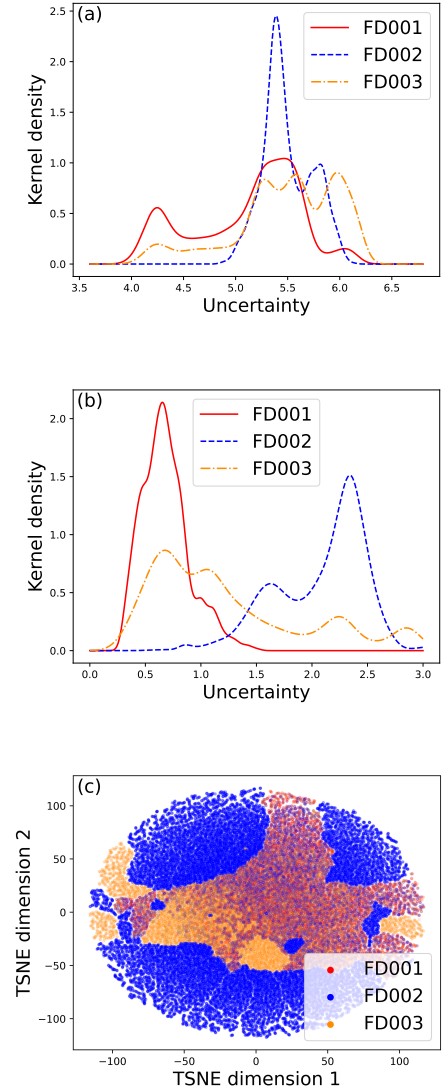


Fig. 2: Kernel density plots of aleatoric uncertainties in (a) and epistemic uncertainties in (b) over test sets from folder FD001, FD002, and FD003 when predicted over ensemble model trained on FD001. The uncertainties of FD001 are plotted in a red solid line, FD002 in the dashed blue line, and FD003 in a dash-dotted orange line. (c) shows TSNE embedding where projections of data on TSNE dimension 1 and TSNE dimension 2. The data from different data-sets is provided in different colors red for FD001, blue for FD002, and orange for FD003.

In Fig. 2 (a) we see that the aleatoric uncertainties lie in the same region for all 3 data-sets. This indicates that the uncertainties coming from the system are similar in the three data-sets. This is because the model was trained to predict the aleatoric uncertainties (σ of the estimates) of FD001 and therefore model predicates aleatoric uncertainties in the same region as FD001. These uncertainties can only be trusted

TABLE II: Table showing the comparison of our method with state-of-the-art methods on point prediction metrics and probabilistic metrics. The direction of the arrow indicate what makes better model lower or higher. The approaches on the top are point prediction methods and the approaches in the bottom are probabilistic methods. They are separated by a double line.

Method	Point Prediction		Probabilistic Prediction		Reference
	RMSE↓	S↓	PICP↑	NMPIW↓	
RULCLIPPER	13.266	216.0			[15]
MODBNE	15.039	334.2			[16]
Embed-LR1	12.449	219.0			[17]
BiLSTM-ED	14.741	273.0			[18]
TSCG	17.438	468.5			[19]
SBI-EN	13.583	228.0			[20]
MCLSTM	13.711	315.0			[21]
Deep LSTM	16.14	338.0			[4]
Trend_CNN	13.99	336.0			[5]
MC-dropout	13.06	-	-	-	[11]
LSTMBS	14.481	481.1	0.960	0.377	[22]
IESGP	14.720	331.9	0.995	0.540	[23]
Lognorm-LSTM(Mean)	12.227	243.8	0.950	0.316	[10]
Our Method (Mean)	15.01	417.0	0.956	0.473	

when the epistemic uncertainties are low. These aleatoric uncertainties are due to inherent characteristics of data and can not be reduced by any means.

Finally, to compare against the existing state-of-the-art point-prediction approaches, we evaluated our approach using point-prediction and probabilistic metrics. The comparison is shown in Table. II. In this work, the focus is on how to include probabilistic prediction in RUL modeling and use a simple LSTM model for RUL predictions. From the table, we see that our simple RUL-LSTM compares well with state-of-the-art point prediction models. Moreover, our probabilistic approach can be easily implemented in the best performing RUL predictive models.

VI. CONCLUSION

To summarise, we proposed an ensemble LSTM neural network for probabilistic prediction to incorporate both aleatoric and epistemic uncertainties for RUL prediction. This approach is tested on NASA’s turbofan jet engine CMAPSS data-set. Our results show how epistemic and aleatoric uncertainties can be added to RUL predictions. The knowledge of the uncertainties, especially the epistemic uncertainty, allows us to estimate the ensemble model prediction confidence on a given data-set. If the epistemic uncertainty is large, then it is a strong indication that the ensemble model has not seen this data before and needs to be re-trained for this data-set. This ensemble probabilistic approach is simple to implement on already existing RUL point-predictions, which would significantly improve trust and transparency to current state-of-the-art predictions.

Further work could explore methods for the selection of optimal distribution in place of Gaussian distribution based on the data and could perform further tests to understand the effect of number of models in the ensemble.

ACKNOWLEDGMENT

This work is supported by VINNOVA FFI under the contract 2020-05138. We thank Kuo-Yun Liang for helping us by reviewing this work. Finally, thanks to Scania CV AB for supporting this research project.

REFERENCES

- [1] Y. Lei, N. Li, S. Gontarz, J. Lin, S. Radkowski, and J. Dybala, “A model-based method for remaining useful life prediction of machinery,” *IEEE Transactions on reliability*, vol. 65, no. 3, pp. 1314–1326, 2016.
- [2] M. Tan and Q. Le, “Efficientnetv2: Smaller models and faster training,” in *International conference on machine learning*. PMLR, 2021, pp. 10 096–10 106.
- [3] W. X. Zhao, K. Zhou, J. Li, T. Tang, X. Wang, Y. Hou, Y. Min, B. Zhang, J. Zhang, Z. Dong *et al.*, “A survey of large language models,” *arXiv preprint arXiv:2303.18223*, 2023.
- [4] S. Zheng, K. Ristovski, A. Farahat, and C. Gupta, “Long short-term memory network for remaining useful life estimation,” in *2017 IEEE international conference on prognostics and health management (ICPHM)*. IEEE, 2017, pp. 88–95.
- [5] L. Fan, Y. Chai, and X. Chen, “Trend attention fully convolutional network for remaining useful life estimation,” *Reliability Engineering & System Safety*, vol. 225, p. 108590, 2022.
- [6] V. P. Nemani, H. Lu, A. Thelen, C. Hu, and A. T. Zimmerman, “Ensembles of probabilistic lstm predictors and correctors for bearing prognostics using industrial standards,” *Neurocomputing*, vol. 491, pp. 575–596, 2022.
- [7] E. Hüllermeier and W. Waegeman, “Aleatoric and epistemic uncertainty in machine learning: An introduction to concepts and methods,” *Machine Learning*, vol. 110, pp. 457–506, 2021.
- [8] A. Saxena, K. Goebel, D. Simon, and N. Eklund, “Damage propagation modeling for aircraft engine run-to-failure simulation,” in *2008 international conference on prognostics and health management*. IEEE, 2008, pp. 1–9.
- [9] A. Muneer, S. M. Taib, S. Naseer, R. F. Ali, and I. A. Aziz, “Data-driven deep learning-based attention mechanism for remaining useful life prediction: Case study application to turbofan engine analysis,” *Electronics*, vol. 10, no. 20, p. 2453, 2021.
- [10] K. T. Nguyen, K. Medjaher, and C. Gogu, “Probabilistic deep learning methodology for uncertainty quantification of remaining useful lifetime of multi-component systems,” *Reliability Engineering & System Safety*, vol. 222, p. 108383, 2022.

- [11] M. Mitici, I. de Pater, A. Barros, and Z. Zeng, "Dynamic predictive maintenance for multiple components using data-driven probabilistic rul prognostics: The case of turbofan engines," *Reliability Engineering & System Safety*, vol. 234, p. 109199, 2023.
- [12] B. Lakshminarayanan, A. Pritzel, and C. Blundell, "Simple and scalable predictive uncertainty estimation using deep ensembles," *Advances in neural information processing systems*, vol. 30, 2017.
- [13] A. Malinin, B. Mlodozeniec, and M. Gales, "Ensemble distribution distillation," *arXiv preprint arXiv:1905.00076*, 2019.
- [14] X. Zhang, P. Xiao, Y. Yang, Y. Cheng, B. Chen, D. Gao, W. Liu, and Z. Huang, "Remaining useful life estimation using cnn-xgb with extended time window," *IEEE Access*, vol. 7, pp. 154 386–154 397, 2019.
- [15] E. Ramasso, "Investigating computational geometry for failure prognostics in presence of imprecise health indicator: Results and comparisons on c-mapss datasets," in *PHM Society European Conference*, vol. 2, no. 1, 2014.
- [16] C. Zhang, P. Lim, A. K. Qin, and K. C. Tan, "Multiobjective deep belief networks ensemble for remaining useful life estimation in prognostics," *IEEE transactions on neural networks and learning systems*, vol. 28, no. 10, pp. 2306–2318, 2016.
- [17] V. T. Narendhar Gugulothu, P. Malhotra, L. Vig, P. Agarwal, and G. Shroff, "Predicting remaining useful life using time series embeddings based on recurrent neural networks," *International Journal of Prognostics and Health Management*, vol. 9, 2018.
- [18] W. Yu, I. Y. Kim, and C. Mechefske, "Remaining useful life estimation using a bidirectional recurrent neural network based autoencoder scheme," *Mechanical Systems and Signal Processing*, vol. 129, pp. 764–780, 2019.
- [19] H. Xu, N. Fard, and Y. Fang, "Time series chain graph for modeling reliability covariates in degradation process," *Reliability Engineering & System Safety*, vol. 204, p. 107207, 2020.
- [20] W. Yu, I. Y. Kim, and C. Mechefske, "Remaining useful life estimation using a bidirectional recurrent neural network based autoencoder scheme," *Mechanical Systems and Signal Processing*, vol. 129, pp. 764–780, 2019.
- [21] S. Xiang, Y. Qin, J. Luo, H. Pu, and B. Tang, "Multicellular lstm-based deep learning model for aero-engine remaining useful life prediction," *Reliability Engineering & System Safety*, vol. 216, p. 107927, 2021.
- [22] Y. Liao, L. Zhang, and C. Liu, "Uncertainty prediction of remaining useful life using long short-term memory network based on bootstrap method," in *2018 IEEE international conference on prognostics and health management (ICPHM)*. IEEE, 2018, pp. 1–8.
- [23] C. Liu, L. Zhang, Y. Liao, C. Wu, and G. Peng, "Multiple sensors based prognostics with prediction interval optimization via echo state gaussian process," *IEEE Access*, vol. 7, pp. 112 397–112 409, 2019.